

Article

Estimation of the Average Retention Time of Precipitation at the Surface of a Catchment Area for Lake Biwa

Maho Iwaki ^{1,*}, Yosuke Yamashiki ², Takashi Toda ¹, Chunmeng Jiao ³ and Michio Kumagai ⁴¹ Lake Biwa Museum, Oroshimo, Kusatsu 606-8501, Japan; toda-takashi@biwahaku.jp² Graduate School of Advanced Integrated Studies in Human Survivability, Kyoto University, Kyoto 606-8306, Japan; yamashiki.yosuke.3u@kyoto-u.ac.jp³ Lake Biwa Environmental Research Institute, Otsu 520-0022, Japan; jiao-c@lberi.jp⁴ Lake Biwa Sigma Research Center, Ritsumeikan University, Kyoto 525-8577, Japan; mkt24354@se.ritsumei.ac.jp

* Correspondence: iwaki.maho.28n@kyoto-u.jp; Tel.: +81-90-3896-6758

Abstract: In a lake catchment system, we analyzed the lake water-level responses to precipitation. Moreover, we identified the average precipitation retention time—due to subsurface flows—from the delay time calculated using the response function with data of water level and catchment precipitation (both rainfall and snowfall) collected over 30 years of continuous observations of Lake Biwa, Japan. We focused on the snow reserves and the water-level response delay due to the snowmelt of Lake Biwa catchment. We concluded that the average precipitation retention time of the catchment subsurface flow (i.e., above the impermeable layer) in Lake Biwa was approximately 45 days. Additionally, the precipitation retention time during snowmelt was shorter than that during the dry season. Overall, the shape of the response function reflects the lake system. This knowledge improves the understanding of lake systems and can be helpful for lake resource managers. Furthermore, finding the delay time from the response function may be useful for determining the contribution of rainfall to increasing the water levels of other lakes. Therefore, our results can contribute to the development of management strategies to address inland aquatic ecosystems and conservation.

Keywords: lake water level; precipitation retention time; impulse response function; subsurface flow; snow water equivalent; snowmelt; climate change; Lake Biwa



Citation: Iwaki, M.; Yamashiki, Y.; Toda, T.; Jiao, C.; Kumagai, M. Estimation of the Average Retention Time of Precipitation at the Surface of a Catchment Area for Lake Biwa. *Water* **2021**, *13*, 1711. <https://doi.org/10.3390/w13121711>

Academic Editor: Anas Ghadouani

Received: 30 April 2021

Accepted: 16 June 2021

Published: 21 June 2021

Publisher's Note: MDPI stays neutral with regard to jurisdictional claims in published maps and institutional affiliations.



Copyright: © 2021 by the authors. Licensee MDPI, Basel, Switzerland. This article is an open access article distributed under the terms and conditions of the Creative Commons Attribution (CC BY) license (<https://creativecommons.org/licenses/by/4.0/>).

1. Introduction

Climate change can directly and indirectly impact watershed dynamics, nutrient loads, thermal structures, salinity regimes, pollutant dynamics, methane emissions, sedimentation processes, and inland aquatic ecosystems [1]. Lakes in arid or semi-arid areas are particularly vulnerable to climate change due to the limited water availability. For such regions, drivers of water shortage include increased water withdrawal during droughts and intensified agricultural use in the contributing catchment [1]. Many works have been devoted to study water-level changes in dry regions of Aral Sea [2,3], Lake Kinneret [1,4,5], Lake Urmia [6–9], and Lake Abert [10]. Many other lakes in arid areas are also reportedly shrinking and disappearing, presenting severe global issues [2,3,5]. While water storage is already an acute problem for lakes in arid areas, this problem is also receiving increasing attention for wet subtropical lakes due to changes in the water cycles caused by climate change.

Natural water-level fluctuations are an inherent feature of lake ecosystems, and a small change in water-level patterns could impact shoreline ecosystems [11] and a range of ecosystem services. For example, water-level dynamics are important for the survival of many species that have evolved synchronized life cycles to such fluctuation patterns [4,12–14]. Thus, the impact of water-level fluctuations in lake dynamics is important for ecosystems [15–17]. Lake Biwa is a large, deep subtropical lake located in central Japan; its

outflow is controlled by underflow gates that are managed according to operation regulations for water supply, as well as hydropower, ensuring the maintenance of a certain water level that is conducive for fish breeding but prevents floods. The seasonal changes in the lake's water level are important for the littoral zone ecosystem and the spawning habitats of endemic fish species [18–21]. Climate adaptive water-level management that helps to protect valuable habitats benefits from better knowledge of dynamic response relationships between precipitation and water-level changes.

The average retention time of precipitation at a subsurface of a catchment area and the duration it might take to affect lake levels can be estimated by calculating a response time of lake levels from given precipitation events [22]. The water level of a lake represents the balance of various forms of inputs and outputs, and each element has a unique temporal and spatial frequency scale. Although lake water-level fluctuation is complex, changes are often considered to occur linearly; in other words, a complex water-level fluctuation is a consequence of additive water balancing effects [4,23]. Therefore, individual mechanisms can be separated when divided by their frequencies when inherent oscillations for individual contributing phenomena are assumed. Impulse response functions describe the causal relationships between the input and output factors. They can be used to determine the time delay it takes for precipitation in the catchment to take effect on the water level of water bodies [22]. In hydrology, this method has been successfully applied to rivers and groundwater [24–26], but not to lakes.

The dynamics of water levels in Lake Biwa are complex due to its large (surface area of 670.25 km²) and complex catchment characteristics. Frequency analysis at the sub-annual scale may be an effective analytical approach to understand the seasonal-scale response of water levels to the climate. Factors directly affecting the changes in the water level include wind and waves (seconds–minutes), seiches (minutes–hours), rainfall (direct–months), river outflows (minutes–days), evaporation (direct–months), groundwater flux (days–years), and other factors such as direct water extraction. Over a short-term timescale of several days, heavy rainfall was found to have the strongest effect on water-level changes [23]. While rainfall on the lake's surface directly contributes to the change in levels, rainfall on the catchment can take a long time (~months via subsurface, and ~years via groundwater) to take an effect.

In this paper, we examined the time lag between precipitation events and the subsequent water level changes to determine how a series of precipitation events produces the effects on water level. This helped clarify the causal relationships not explained in previous research. In this study, we aimed to conduct a frequency-based analysis of the medium-term water-level changes of Lake Biwa to physically analyze the medium-term changes. We considered timescales inherent to the factors responsible for the water-level changes to identify the specific factors implicated in the medium-term changes.

2. Methods

2.1. Site Information

Lake Biwa is the largest freshwater resource in Japan, with a surface area of 670.25 km² and a maximum depth of 104.1 m [27]. The catchment area of 3174 km² gives it a combined water and land surface area of 3848 km². Approximately one-third of this area is a plain that is generally <200 m high, i.e., <120 m above the lake surface (Figure 1). The northeast of Lake Biwa is bounded by the Ibuki Mountains, with an elevation of over 800 m. The lake is divided into two basins; the North Basin is wide and deep, while the South Basin is narrower and much shallower (Figure 1). The surface area and mean water depth of the North Basin are 618.65 km² and 43 m, respectively, while those of the South Basin are 51.60 km² and 4 m, respectively [28].

- ▲ Water-level data ($\Delta t = 1$ day)
Lake Biwa Work Office (Ministry of Land Infrastructure, Transport and Tourism)
- Meteorological data ($\Delta t = 1$ day) Automated Meteorological Data Acquisition System (AMeDAS), Japan Meteorological Agency
- ◆ Discharge data ($\Delta t = 1$ day)
Ministry of Land Infrastructure, Transport and Tourism, Waterworks Bureau, City of Kyoto, Kansai Electric Power Corporation.
- Snow water equivalent (1–2 times/week)
- ⊙ The water temperature and dissolved oxygen (DO) (1time/2week) at eight depths

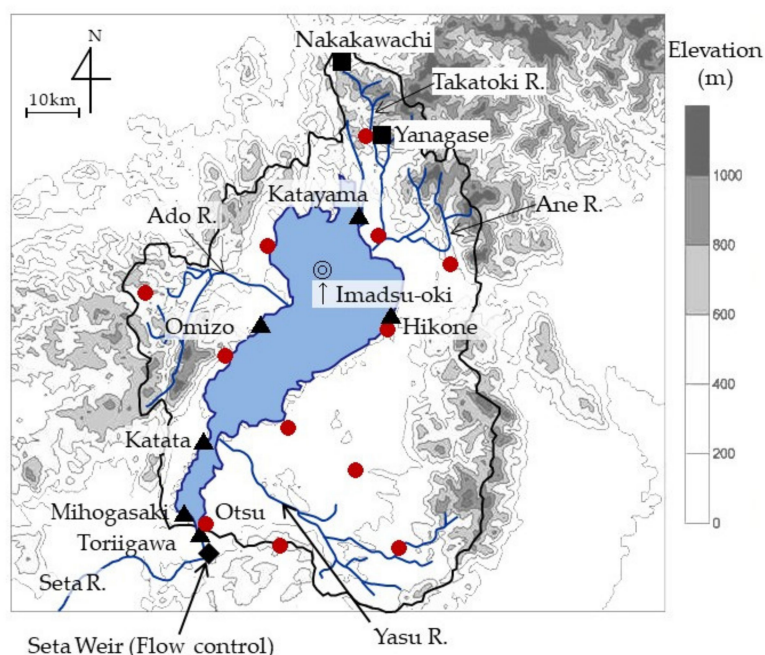


Figure 1. Lake Biwa and its catchment area, with main inflowing rivers and major outflow (Seta River), as well as the locations of water-level and discharge gauges, and meteorological stations. Observation points of the snow water equivalent. These two points were in the same catchment area of the Ane River.

The catchment area of Lake Biwa is located along the boundary region between the Sea of Japan climatic zone (which experiences heavy precipitation in winter) and the Pacific Ocean climatic zone (which experiences a small amount of precipitation in winter), thereby leading to wildly fluctuating weather conditions from year to year. More than 450 rivers and streams flow directly into the lake, but there is only one natural outlet, the Seta River. The Seta River discharge is controlled by the opening and closing of multiple weirs. Its outflow is kept constant over a certain period, and, in such situations, it is suitable for estimating the delay time by using the response function.

To maintain the water level to some extent (e.g., fish breeding to prevent drying of eggs and to prevent floods by typhoons), the ranges are determined by administrative rules. The higher limit of the water level of Lake Biwa was assumed to be the standard water level of +0.3 m except during the flood period (15 June to 15 October), and the lower limit of the water level is set to the following values for two different periods: for June 16 to August 31 every year, it is -0.2 m; for September 1 to October 15 every year, it is -0.3 m [18–21]. The outflow from Lake Biwa is managed according to operation rules. The water levels of Lake Biwa are adjusted so that levels are between -0.3 and $+0.3$ m, and if the level exceeds this value, the water levels are decreased to $+0.3$ m for flood control as soon as possible. The volume of water discharged from Lake Biwa through the Seta River is controlled by the opening and closing of multiple weirs, and these stabilize the discharge to a relatively fixed rate; when the amount of discharge change is too large, especially after heavy rainfall, the discharge can be increased if necessary. Water levels are managed to support the spawning and hatching period of spring-breeding fish from March to June, as well as to support agricultural water use from June to September. During September–December, which is another spawning season for fish, water levels are not adjusted excessively. The influence of rainfall on the water level of Lake Biwa is reduced by artificially increased outflows. Various changes in the outflow amounts are achieved via weir operation. These changes take place over several hours to avoid an abrupt change within the range of $20\text{--}700\text{ m}^3\cdot\text{s}^{-1}$, which then has to be incorporated into the calculations of the water-level data. The effects of weir operation include the following: the reflection of the flow hardly reached the north basin due to topographic differences, while inverse flow

was observed from the south to north (e.g., density currents, strong typhoon); however, these are not induced by the operation of weirs [19,29].

2.2. Water Flow from the Catchment Area to Lake Biwa and Its Water Balance

We focused on the snow accumulation/snowmelt process of water flow and analyzed the average retention time of precipitation at the surface of a catchment area for Lake Biwa, the schematic of which is shown in Figure 2. We standardized the output for water-level data in the lake obtained through rainfall (input) from 1 January 1983 to 31 December 2013, and we calculated the response function on the basis of the autocorrelation function of the input precipitation data (rainfall) and the cross-correlation of the input and output (water level) data.

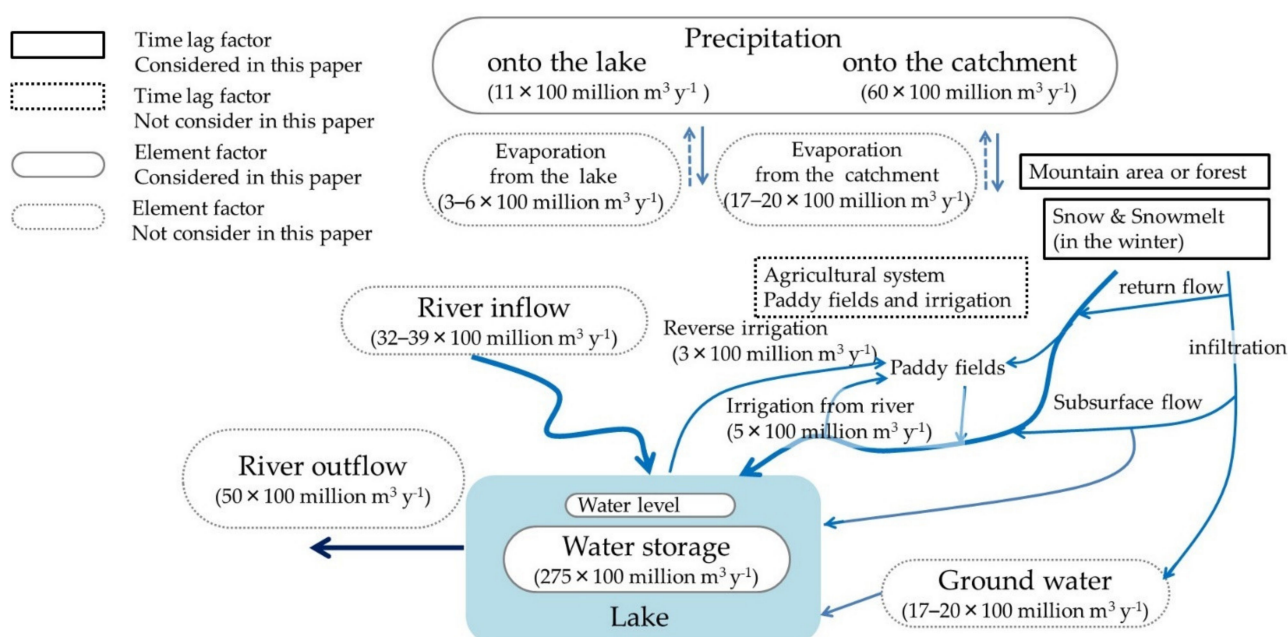


Figure 2. Schematic model showing the water flow from the catchment area to Lake Biwa and its water balance. The values of water balance are cited from [30–32].

To determine the precipitation retention time in the surface of the catchment area, we were required to simplify the calculations and neglect the changes in some factors (Figure 2). In humid areas, the changes in the lake surface area were small, and the seepage of groundwater into the lake was very slow; additionally, the ratio of evaporation to outflow in Lake Biwa was estimated to be $\sim 2\%$ [30,31]. The variation in evaporation was detected using fast Fourier transform (FFT) as the data had a clear periodicity. Unlike arid areas, the water level of Lake Biwa does not change significantly with daily evaporation [33,34]. Therefore, factors that cause changes in deep groundwater recharge and the evaporation of water from the lake surface were excluded from our calculations; the impact was not considered due to the above.

2.3. Data Acquisition

2.3.1. Water Level

The water levels of Lake Biwa have been measured since 4 February 1874, and they were most recently measured by the Ministry of Land, Infrastructure, Transport, and Tourism (MLIT). We used daily water-level measurements of Lake Biwa from 1 January 1983 to 31 December 2013, obtained at 6:00 a.m. every day, representing the water height relative to the Lake Biwa baseline of $\pm 0 \text{ m}$ (BSL: Biwako standard level; $+84.371 \text{ m}$) [32]. Until March 1992, the water level was based on the level at the Toriigawa observation point

(Figure 1). After 1992, the average water level of five observation points (Katayama, Omizo, Hikone, Katata, and Mihogasaki; Figure 1) was used as the water level of Lake Biwa.

2.3.2. Outflow from Lake Biwa

There are four outlets in Lake Biwa: one major river discharge, two canal discharges, and one minor channel withdrawal for a hydropower station. The only natural river discharge from the lake is the Seta River, where the daily flow record was provided by MLIT. Discharge observations through the two canals and the channel of the hydropower station were provided by the Waterworks Bureau, the City of Kyoto, and the Kansai Electric Power Corporation. The volume of water discharged from Lake Biwa through Seta River is controlled by the opening and closing of the multiple weirs. Since 1972, the peak water level has been controlled to stay roughly at BSL. River discharge changes when the weirs open and close, and then settles down to a fixed rate. Because discharge rates fluctuate between 20 and 700 $\text{m}^3 \cdot \text{s}^{-1}$, theoretical changes in the water level of the lake over the course of a day can be 3, 32, and 90 mm when the discharge rates are 20, 250, and 700 $\text{m}^3 \cdot \text{s}^{-1}$, respectively. The other two discharges are canals for water supply to Kyoto city and a waterway to the Uji Power Plant; the fixed discharge rate is less than 30 $\text{m}^3 \cdot \text{s}^{-1}$.

2.3.3. Precipitation

We used daily (accumulated) precipitation values from 12 observation points that exist in catchment areas from 1 January 1983 to 31 December 2013 (Figure 1). Meteorological data were provided from the Japan Meteorological Agency (JMA). However, accurate snowfall measurements were not recorded by the rainfall gauges during the winters. The type of rain gauge is standard, which is essentially one that keeps accumulating water until it is measured and is emptied automatically. The resolution of this rain gauge was determined to be 0.5 mm from the tipping-bucket volume. The rain gauges were connected to a data logger that recorded their pulse outputs. This type of rain gauge has some time lag in snowfall and snowmelt season. To compensate for this lack of information, we used daily snow depth change from three observation points, published by the JMA (Figure 1).

2.3.4. Snow Density and Snow Water Equivalent

The snow depth was converted to the water volume (precipitation) using the snow density. We carried out field observations during the winter of 2001 to calculate this snow density. In addition, we used data from 16 surveys. In these surveys, snow conditions, depth, and weight were obtained, as shown in Table 1 (only for the snowmelt season). The average snow density was calculated from the snow weight and height. During the snowmelt season in this region, we used the average snow density as approximately 0.43 kg m^{-3} to calculate the equivalent precipitation (Table 1). The amount of snowfall was calculated as follows:

$$\text{Daily Snowfall (kg m}^{-2}\text{)} = \text{snow density (kg m}^{-3}\text{)} \times \Delta \text{ snow depth (m)}.$$

$$\text{Precipitation} = \text{rainfall} + \text{snowfall}.$$

Table 1. Observed average snow density at the north catchment area of Lake Biwa during the winter of 2001[†].

Date	Weather	Snow Depth (cm)	Snow Water Equivalent (mm)	Snow Density ($\text{kg} \cdot \text{m}^{-3}$)	Air Temperature ($^{\circ}\text{C}$)	Surface Snow Temperature ($^{\circ}\text{C}$)
24 February 2002	Sunny	82.6	36.5	0.442	2.9	−1.0
28 February 2002	Cloudy	74.6	32.9	0.441	1.7	−0.9
5 March 2002	Cloudy	59.4	25.9	0.436	1.5	−2.1
14 March 2002	Rainy	20.5	8.6	0.418	5.4	−2.2
17 March 2002	Sunny	10.1	4.6	0.454	13.2	−3.0

[†] Only the snowmelt season is shown (cited [35], Figure 1).

We also refer to the snow water equivalent observed in the northern catchment area of Lake Biwa from 2009 to 2010. We carried out snowfall observations at two points (near-mountain area and mountain area) in the catchment area of Lake Biwa (Figure 1) during the winter of 2009/2010. The snow conditions, depth, and weight were measured in these surveys.

2.3.5. Dissolved Oxygen and Water Temperature

Dissolved oxygen (DO) levels and water temperature dynamics were used to justify the calculated delay times for snowmelt impacts on the lake. The water temperature and DO levels measured in Lake Biwa from 2009 to 2010 by the Lake Biwa Environmental Research Institute were also taken into account; these measurements were conducted every 2 weeks at eight depths in the northern part of the lake at the center of Imadsu-oki (Figure 1; [36]).

2.4. Impulse Response Function

One of the most important decisions regarding the use of the response function of endorheic and exorheic lakes is the shape of the response function. The shape of the response function reflects the lake system itself, and such knowledge enables a better understanding of lake systems and dominant processes within lakes to be obtained. Such information will further be helpful to lake resource managers. In contrast, wavelet transformation is a good method for identifying the change in periods, since it does not lose information on time when used in the frequency domain. However, we did not conduct wavelet transformation; there were many factors to consider. We first needed to identify and separate some of the more complex factors; wavelet transformation was the next step.

For calculating the response function, $x(t)$ signifies the rainfall at a certain location representative of the lake's watershed, and $y(t)$ indicates the lake level; both $x(t)$ and $y(t)$ are functions of time. We assumed that $y(t)$ could be described as a function of the integral of $x(t)$ ($t \leq 0$). More specifically, $y(t)$ is the sum of the product of the past precipitation, $x(t - \tau)$, multiplied by the impulse response function, i.e., $h(\tau)$. Thus,

$$y(t) = \int_0^{+\infty} x(t - \tau)h(\tau)d\tau, \quad (1)$$

where τ is the time lag. Because $h(\tau)$ specifies the relationship of $x(t)$ and $y(t)$, it should reflect the process of how the lake level is affected by rainfall [37]. Here, $h(\tau)$ was determined using Equation (1) as an integral equation, as shown in the flow chart for calculating the response function (Appendix A) [22].

Since $y(t)$ and $x(t)$ are observable values, we can find $h(\tau)$ by solving Equation (1) as an integral equation. The impulse response function can also be explained as the response to the unit impulse; thus, in case $x(t) = \delta(t)$ in Equation (1), $y(t)$ is equal to $h(t)$, where $\delta(t)$ is the delta function. The strict definition of the delta function is rather complicated, but it can be roughly defined as

$$\delta(t) \begin{cases} = 0 & (t \neq 0) \\ = \infty & (t = 0) \end{cases} \quad \text{and} \quad \int_{-\infty}^{\infty} \delta(t)dt = 1.$$

We then estimated the response function $h(\tau)$ through the mutual correlation function.

$$C_{xy}(\tau) = \overline{x(t)y(t+\tau)} = \int_{-\infty}^{+\infty} h(\eta)\overline{x(t)x(t+\tau-\eta)}d\eta, \quad (2)$$

where the overbar stands for the ensemble mean. Moreover, the autocorrelation function is defined as

$$C_{xx}(\tau) = \overline{x(t)x(t+\tau)}. \quad (3)$$

Therefore,

$$C_{xy}(\tau) = \int_{-\infty}^{+\infty} h(\eta)C_{xx}(\tau - \eta)d\eta. \quad (4)$$

The complex Fourier transformation of the mutual correlation function $C_{xy}(\tau)$ is the cross-spectrum,

$$S_{xy}(\omega) = \frac{1}{2\pi} \int_{-\infty}^{+\infty} C_{xy}(\tau)e^{-i\omega\tau}d\tau, \quad (5)$$

and the autocorrelation function $C_{xx}(\tau)$ is the power spectrum,

$$S_{xx}(\omega) = \frac{1}{2\pi} \int_{-\infty}^{+\infty} C_{xx}(\tau)e^{-i\omega\tau}d\tau. \quad (6)$$

The cross-spectrum can be rewritten as

$$\begin{aligned} S_{xy}(\omega) &= \frac{1}{2\pi} \int_{-\infty}^{+\infty} C_{xy}(\tau)e^{-i\omega\tau}d\tau = \frac{1}{2\pi} \int_{-\infty}^{+\infty} \int_{-\infty}^{+\infty} h(\eta)C_{xx}(\tau - \eta)e^{-i\omega\tau}d\eta d\tau \\ &= \frac{1}{2\pi} \int_{-\infty}^{+\infty} \int_{-\infty}^{+\infty} h(\eta)e^{-i\omega\eta}C_{xx}(\sigma)e^{-i\omega\sigma}d\eta d\sigma \\ &= \frac{1}{2\pi} \int_{-\infty}^{+\infty} h(\eta)e^{-i\omega\eta}d\eta \cdot \frac{1}{2\pi} \int_{-\infty}^{+\infty} C_{xx}(\sigma)e^{-i\omega\sigma}d\sigma \\ &= H(\omega) \cdot S_{xx}(\omega), \end{aligned} \quad (7)$$

where $\sigma = \tau - \eta$, and $H(\omega)$ is the system function (Fourier transformation of $h(\tau)$),

$$H(\omega) = \frac{1}{2\pi} \int_{-\infty}^{+\infty} h(\eta)e^{-i\omega\eta}d\eta, \quad (8)$$

which can be calculated from the cross- and power spectra as follows:

$$H(\omega) = \frac{S_{xy}(\omega)}{S_{xx}(\omega)}. \quad (9)$$

Now, we can find the response function $h(\tau)$ via the reverse Fourier transformation of $H(\omega)$. We used the FFT method to convert $C_{xy}(\tau)$ and $C_{xx}(\tau)$ to $S_{xy}(\omega)$ and $S_{xx}(\omega)$, respectively, as well as to convert $H(\omega)$ to $h(\tau)$ [38].

The key information needed for our response function is the timing of the rainfall events (impulse) and the timing and shape of the water-level changes (response). The positive response function values imply that the output values respond positively to the impulse, i.e., they are positively correlated. To calculate the response functions, $x(t)$ and $y(t)$ were standardized to make the interpretation of $h(\tau)$ easier. The positive values of the τ displacement were used since the response functions were calculated to investigate responses to past events.

By using rainfall as the input and water level as the output, we calculated the cross-correlation function of the input and output and the autocorrelation function of the input. We then conducted a Fourier transformation and converted the results to the frequency domain; we divided the cross-correlation function, $S_{xy}(\omega)$, by the autocorrelation function, $S_{xx}(\omega)$. The positive values of the τ displacement were used as the response functions to investigate responses to past events. We subsequently performed a reverse Fourier transform to return to the time domain and identify the response function [38].

To investigate the influence due to the changes in the water-level observations, we compared the water-level data of Toriigawa (before) and the average of five points (after) from 1993 to 2013 (Figure A2). We conducted a paired two-sided t -test and calculated the value of the coefficient of correlation of Pearson. We first calculated the response function by using records from all 30 years (input data were rainfall data only). Next, we added the snowfall data converted into rainfall data. We used the data as precipitation; then, we compared the response function rainfall water level and precipitation water level. To identify the peaks of the calculated response function, we conducted a test whereby the peak of the response function by the paired two-sided t -test showed that the peak values

and non-peak values did not correspond. This means the average of the peak values and the average of the non-peak values were not the same. Identification of the three peaks (45, 63, and 71 days) was conducted in the same way and verified with the paired two-sided *t*-test with correspondence, which showed that none were significant. These tests conclude that we could use 30 years of water-level data from 1983 to 2013 and could use and discuss the response function calculated using precipitation which included snowfall data converted into rainfall data. Then, we calculated the response functions by using each dataset for a 4 month duration and averaged the 30 year results over each season. The validity of the delay time calculated using the response function was verified using the water temperature, concentration of DO, and observed snow water equivalent, following the procedure outlined in the previous section.

3. Results and Discussion

3.1. Data Assimilation and Calculation of the Response Function

The time series of rainfall (input) and the water level of Lake Biwa (output) are shown in Figure 3. The standard point of BSL changed from Toriigawa to an average of five points (Katayama, Omizo, Hikone, Katata, and Mihogasaki; Figure 1) in 1992. Hence, we calculated two patterns of the response function from 1983 to 2013 (including Toriigawa) and from 1993 to 2013 (average of five points) in Figure 4. In addition, the water-level response functions with respect to the outflow were calculated (Figure 4).

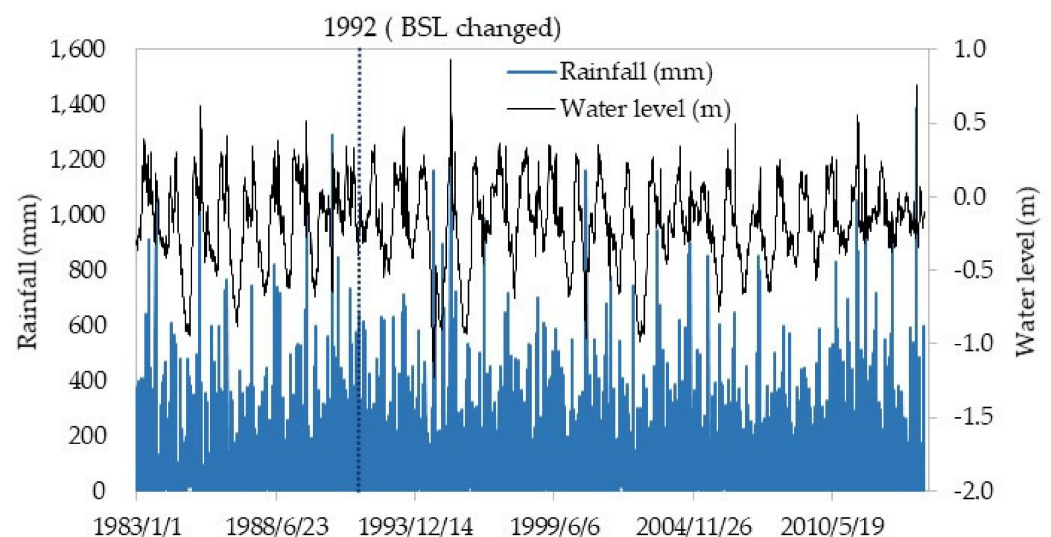


Figure 3. Time series of the input (rainfall) and output (water level of Lake Biwa) data, between 1983 and 2013.

The relationships between the daily water level of Toriigawa and average five points are shown in Figure A2, and the R^2 values were 0.91 from 1993 to 2013 ($m_{\text{Toriigawa}} = 7634$, $n_{\text{5 points}} = 7634$). Subsequently, the two response functions were compared, and their correlations were calculated. We tested whether the correlation coefficients for the two calculated functions were equal, and the value of R^2 was 0.53 (Figure A3).

3.2. Identification of the Peaks Calculated Using the Response Function

The rainfall data did not include the snowfall data, and the effect of snowfall may have been underestimated (Figure 5a). Therefore, we calculated the water-level response function with respect to the average precipitation, as shown in Figure 5b. Until day 131, the shapes of the response functions of rainfall water level and precipitation water level were similar, according to the results of the paired two-sided *t*-test ($R^2 = 0.95$, $m_{\text{Rainfall}} = 130$, $n_{\text{Precipitation}} = 130$, $p < 0.05$) (Figure A4). The response function of rainfall water level became positive approximately on days 1–3 because of the changing river inflow from

the catchment (Figure 5b) [19]. The clearest peaks were obtained on days 45 and 63–71 (Figure 5b).

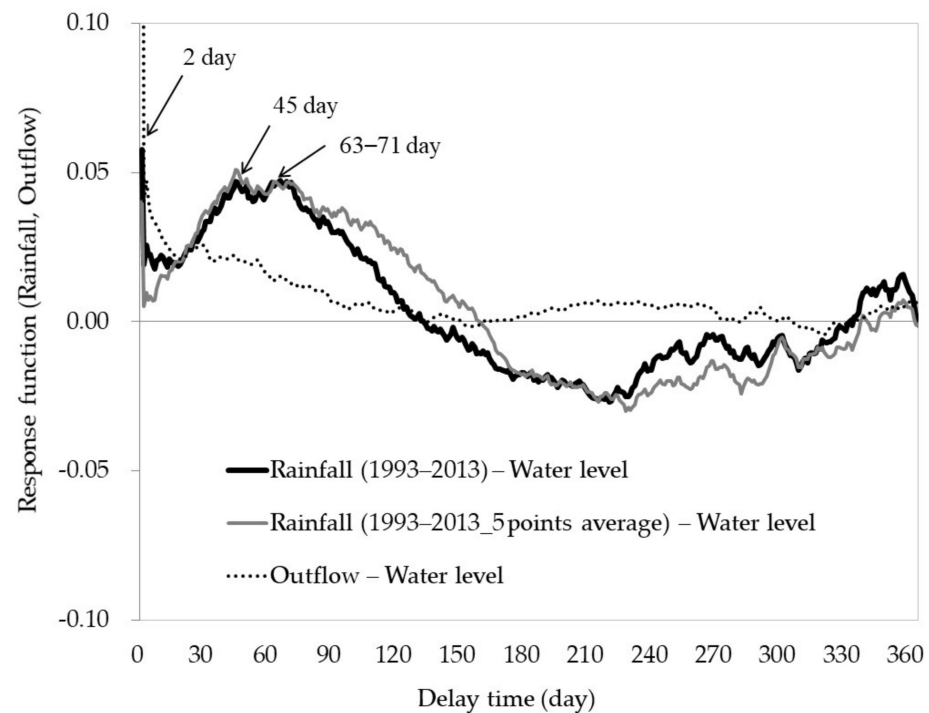


Figure 4. Response functions used for the rainfall water level. All data were standardized.

We conducted a test whereby the peak of the response function during the 30 years (of observation) was calculated on days 45, 63, and 71. The obtained peak and around-peak (before and after the peaks) values were verified with the paired two-sided *t*-test with correspondence; none were significant ($n_{\text{day } 45_{\text{water level}}} = 16$, $n_{\text{day } 63_{\text{water level}}} = 16$, $n_{\text{day } 71_{\text{water level}}} = 16$, $p > 0.05$). This means that the average of the peak and average of the non-peak values were not the same. Therefore, we concluded that the values of the peaks were $\tau = 45$ days, $\tau = 63$ days, and $\tau = 71$ days. Notably, in the data collected over 30 years, a significant difference was observed between the average values of the peaks calculated on days 45 and 71; thus, these were considered to be two different peaks.

3.3. Calculation of the Seasonal Response Function

As for the response functions of the precipitation water level and precipitation water volume, they were calculated for 4 month periods from 1983 to 2013 (Figure 6a,b), and there were 24 results for each season (i.e., 4 months). For example, the figure heading “from January” represents the period from January to April. During the snowfall season in February, a positive peak appeared on day 45 (Figure 6a). The peak value of the response function between February and April (snowmelt season) during the 30 years was identified on day 45. During the snowmelt season, which started in March, two peaks appeared: one on days 28–31 and another on day 56 (Figure 6b). In April, a positive peak appeared on day 56 (Figure 6a,b). Meanwhile, in May, a positive peak appeared on approximately day 45 (Figure 6a). In June, two positive peaks appeared on approximately days 45 and 71. During July and August, a positive peak appeared on approximately day 45. As for September and November, a slight response was detected on approximately days 63–71 (Figure 6a). Lastly, in December and January, slight and weak positive responses were calculated on approximately days 45 and 63 (Figure 6a). In December (snowfall season), two peaks appeared: one on days 28–31 and another on day 56 (Figure 6b).

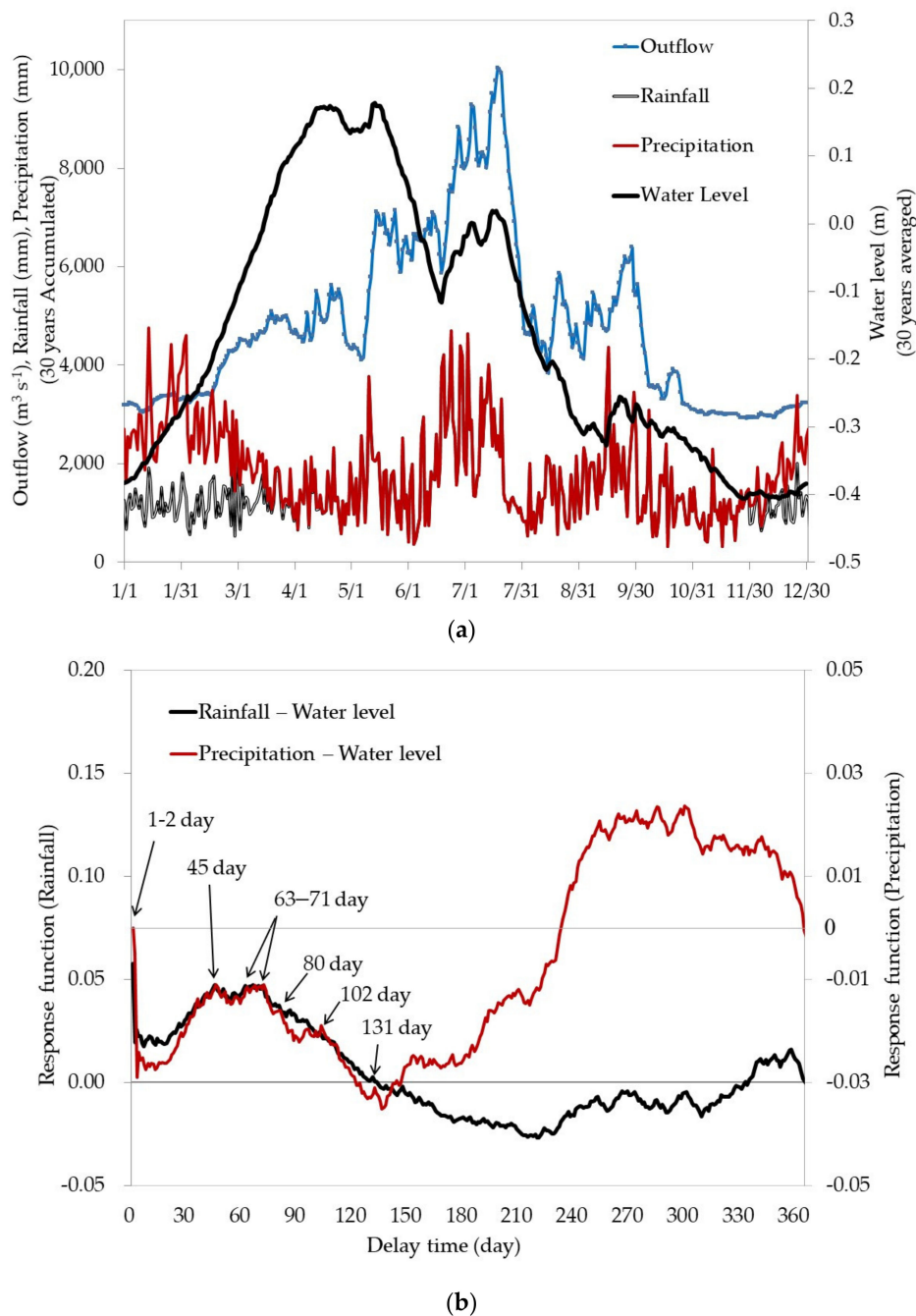


Figure 5. (a) Seasonal water level (averaged), outflow (accumulated), rainfall (accumulated), and precipitation (accumulated) for Lake Biwa and its catchment area, between 1983 and 2013. The average snow density ($0.43 \text{ kg}\cdot\text{m}^{-3}$) was used to convert the snow depth change into snowfall (Table 1). The seasonal outflow traces the change in rainfall. (b) Response functions for the precipitation-water level. All data were standardized and compared with those in Figure 4. The resulting differences represent the effect of snow accumulation and snowmelt.

3.4. Use of the 30 Year Data

We focused on the past 30 years of observations to ensure data quality, consistency, and representativeness of the recent climate. Precipitation and water level are two of the most basic observations made in lakes for water resource management. Although there are data for 140 years of observation for Lake Biwa, we focused on the past 30 years with consistent data quality (e.g., precipitation gauging technologies). In addition, the response function analysis produced a single output (a function), representing all data

being used, and the analysis did not account for any changes or shifts in the system. For the aim of capturing the representative response shapes of the lake and its catchment of recent years, it was ideal to focus on recent decades of data, rather than the full length of available observation.

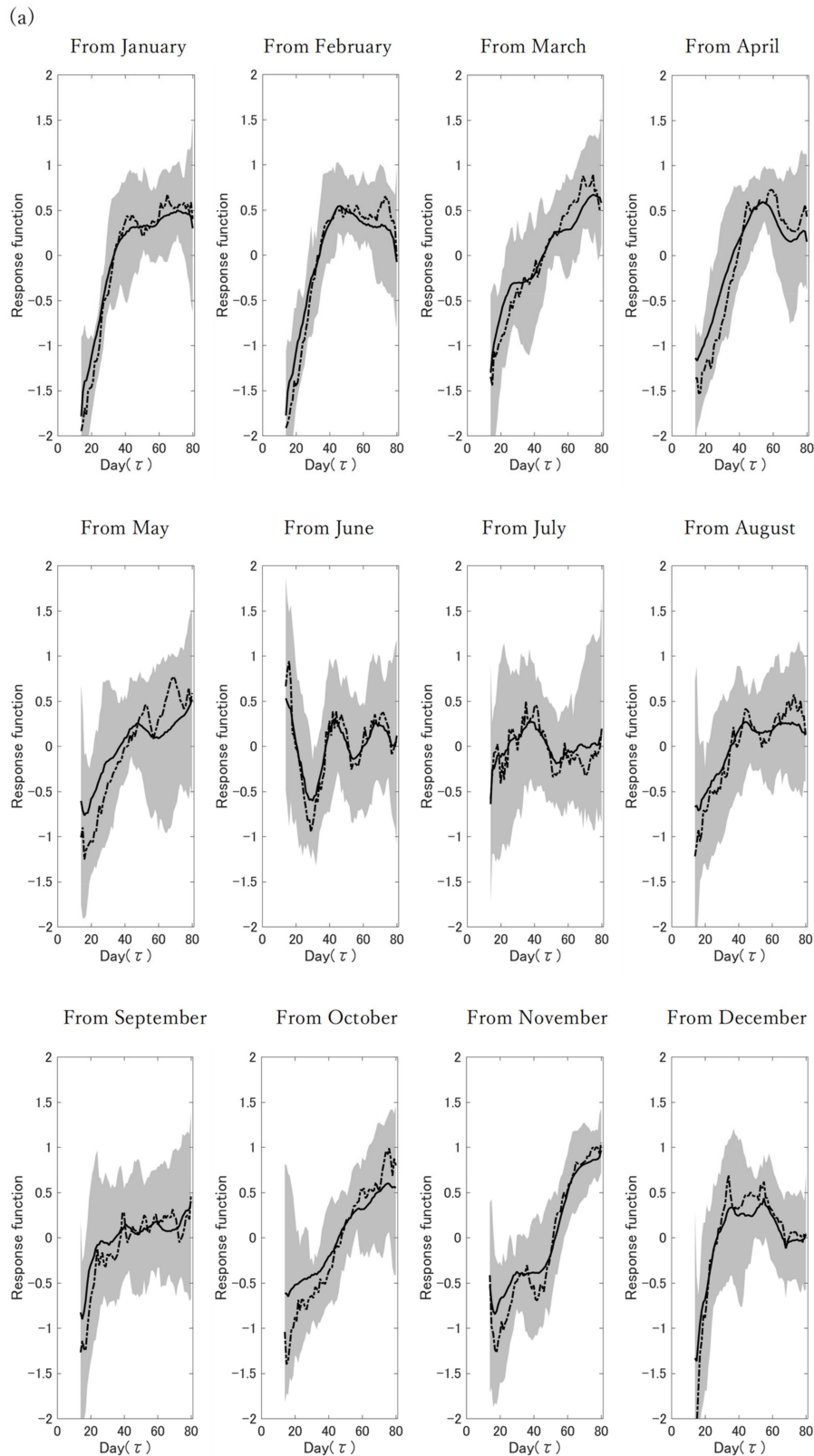


Figure 6. Cont.

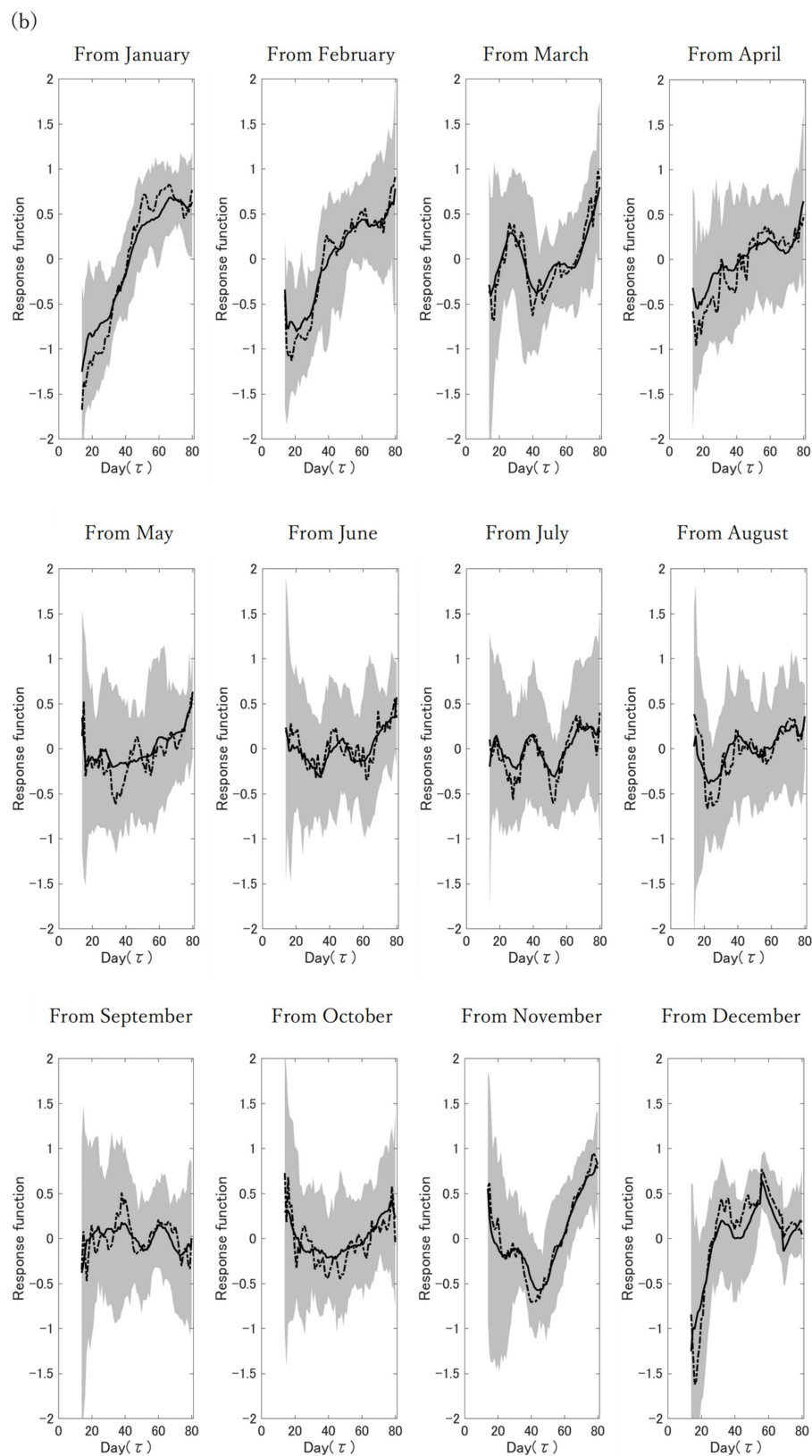


Figure 6. Response functions of (a) the precipitation water level and (b) the precipitation water volume calculated for 4 month periods from 1983 to 2013. The plot under the heading “from January” was from January to April; similarly, all other plots represent 4 month periods. The bold line represents the mean of the calculated response function, and the dotted line represents the median of the calculated response function. The area with hatching lines represents 25–75% of the calculated range.

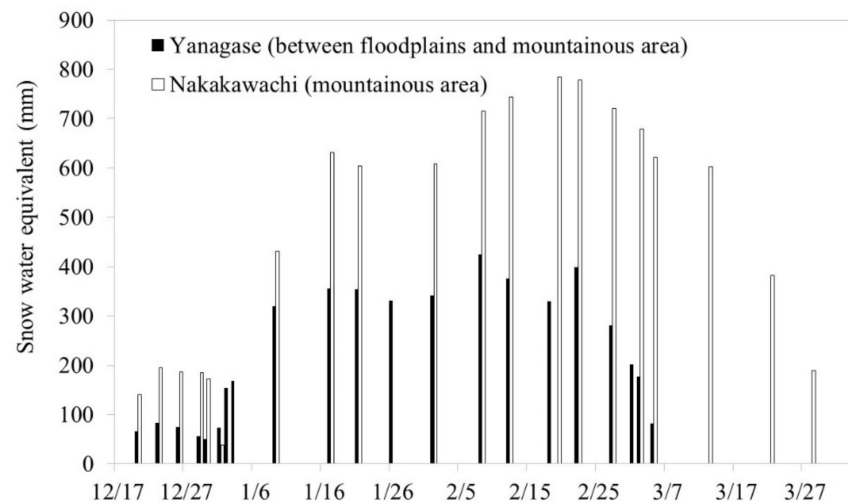
3.5. Inflow Due to Snowmelt Water

We obtained data regarding the snow water equivalent in plain and mountain regions in 2003, 2008, and 2009. We compared these results with the calculated response function (especially clear peaks of 25–35 and 45 days). The clear peak appeared at ~45 days in the snow period, especially in February and March (Figures 5b and 6a). In addition, in the snowmelt season (March), two clear peaks appeared at approximately 25–35 and 45 days in the snowmelt season when the soil was saturated with snowmelt water (Figure 6b). These results suggest that the precipitation retention time during the snowmelt season was shorter than that in other seasons.

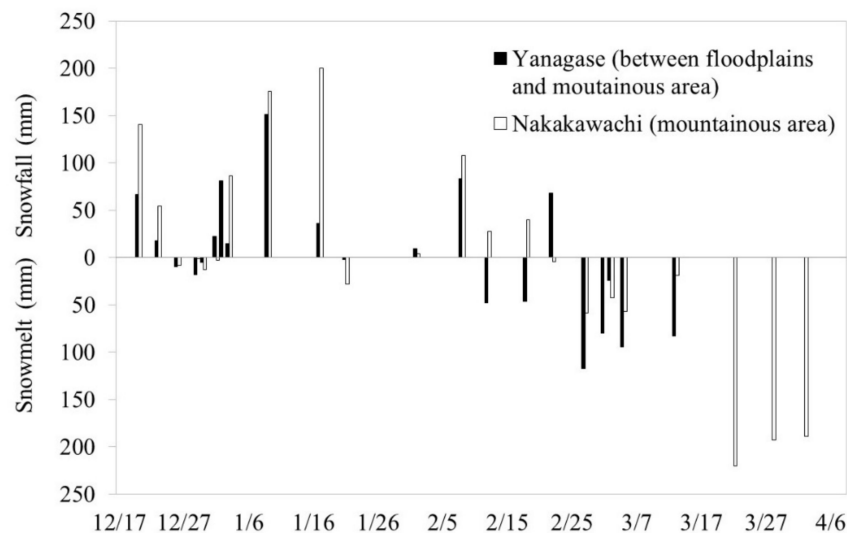
We also discuss the effect of snow accumulation in mountain regions in the winter season. The accumulation of snow in the Lake Biwa drainage basin is unique compared to that in other cold regions, such as Hokkaido and the Tohoku mountains; it is a warm snowy region in which rainfall, snowfall, snowmelt, and snowmelt runoff occur simultaneously, even during the winter. In this region (catchment area of Lake Biwa), snowfall begins in mid-December. In the mountains, a small amount of this snow settles on the ground; however, in the plains, it melts immediately (Figure 7a,b) [39,40]. Peak snowfall occurs from late January to mid-February (Figure 7a). In the plains, the snowmelt that occurs soon after snowfall results in infiltration. In the mid-mountain areas, this occurs only in late February to early March, once the snow has had time to accumulate and after the temperatures increase. In high mountainous areas, snowmelt occurs in late March to early April as temperatures increase even further (Figure 7b). Although this system is extremely complex, efforts have been made to estimate snowmelt volume using various models [40–42]. When the quantity of rainfall considered in the study included the effect of snowfall, two responses (a moderately hilly region and a mountainous region) were possible. The two types of responses could be identified from snow observations collected in the northern Lake Biwa catchment area in 2009 (Figure 7a). In this area, the snow cover period was ~80 days in the moderately hilly region (between plains and mountainous areas) and ~100 days in the mountainous region (Figure 7a,b). These are considered as snow cover delay response times. Herein, according to Figure 5b, there were large peaks around 240–300 days. If the snow cover delay response times were 80–100 days (snow accumulation period) and 25–70 days (approximately retention time) of the maximum retention time caused by snow cover and snowmelt delay (between 105–170 days), it indicated that a longer delay time (around 240–300 days) could have been caused by another factor or process (pathway) of flow into lake, and this must be clarified in the future.

The seasonal data report the occurrence of a positive response in February for approximately 45 days (Figure 6a). From March to April, snowmelt water had a considerable effect; after the release of a considerable amount of water, the time required for the intermediate outflow (including temporary infiltration of the water into the ground, flowing into the rivers, and flowing into the lake) was about 25–35 days. Even outside of the snowmelt season, the positive response took approximately 45 days during the irrigation period (Figure 6a). In addition, during another period, the positive response took 60–70 days (Figure 6a,b). These results suggest that the subsurface flow required a delayed response time of 25–70 days. Therefore, we concluded that the average precipitation retention time of subsurface flow is approximately 45 days in the wet season, 25–35 days in the snowmelt season, and 60–70 days in the dry season.

The calculated delay times were verified using the water temperature and concentration of DO. Before the snowmelt season, the surface water temperature gradually decreased; however, at depths of 60–80 m or at the bottom of the lake, the DO began to recover (i.e., increases again) in winter, when snow fell in December and snowmelt began in February/March (Table 2).



(a)



(b)

Figure 7. Observed snow water equivalent (1–2 times/week) at the north catchment area of Lake Biwa, from December 2009 to March 2010 (Figure 1). (a) Observed seasonal snow water equivalent at Yanagase (between plains and mountainous areas) and Nakakawachi (mountainous area), between December 2009 and March 2010. (b) Seasonal observed snowfall and estimated snowmelt at Yanagase and Nakakawachi, between December 2009 and March 2010 calculated from Figure 7a.

Thermocline deepening can be explained by the observed water temperature (Table 2). The recovery of DO was delayed by approximately 1 month at the deepest point (100 m) compared to that at other depths (Table 2). The observed DO recovery at the lake bottom can be explained by lake mixing; thus far, the DO concentration of snowmelt water from the river is considerably higher than that of the lake. In addition, the snowmelt water from the river is muddy, and the snowmelt water sinks deeper than the surface layer of the lake when it flows out of the river [40–43]. Although the observation interval was 2 weeks, the estimated delay time was approximately 25–35 days. Furthermore, the DO recovery stopped from May 2010; thus, the supply of DO was snowmelt water with a delay of 30–45 days. This result suggested that our estimated delay might be appropriate. Therefore, we concluded that the delay in the recovery of DO, owing to the delay in the

inflow of river water or subsurface flow, is one of the factors that can influence the retention time of the lake.

Table 2. Water temperature and DO [†] levels measured in Lake Biwa from 2009 to 2010 [‡] [36]. The yellow color in the table refers to the deepening of thermocline, indicating the depth of lake mixing.

		Water Temperature (°C)															
Observation Point	Depth\Month-Year	Oct-09		Nov-09		Dec-09		Jan-10		Feb-10		Mar-10		Apr-10		May-10	
The center of Imadsu-oki	0.5 m	22.7	20	17.7	14.6	13.4	11.4	10.0	8.7	8.3	7.9	8.2	8.1	9.1	10.4	14.4	16.8
	5 m	22.6	19.6	17.0	14.6	13.4	11.4	10.0	8.7	8.3	7.9	7.9	8.1	8.6	9.1	12.9	12.9
	10 m	22.6	19.6	17.0	14.6	13.4	11.4	10.0	8.7	8.3	7.9	7.9	8.1	8.2	8.8	12.4	11.1
	15 m	22.2	19.6	16.9	14.6	13.4	11.4	10.0	8.7	8.3	7.9	7.8	8.0	8.2	8.7	11.5	10.6
	20 m	13.9	17.4	16.8	14.6	13.4	11.4	9.9	8.7	8.3	7.9	7.9	7.9	8.2	8.7	11.2	10.1
	30 m	9.8	9.8	10.5	11.2	10.2	11.4	9.9	8.6	8.3	7.9	7.9	7.9	8.2	8.6	9.4	9.4
	40 m	8.8	8.5	8.9	8.8	8.8	10.1	9.9	8.6	8.3	7.9	7.9	7.8	8.2	8.4	8.8	8.9
	60 m	8.3	8.0	8.1	8.2	8.1	8.4	8.8	8.6	8.3	7.9	7.6	7.7	8.0	8.1	8.3	8.5
	80 m	8.2	7.9	7.9	7.9	7.9	8.2	8.3	8.4	8.3	7.7	7.5	7.6	7.6	7.9	8.0	7.9
	Bottom from 1 m	8.1	7.8	7.8	7.9	7.9	8.1	8.2	8.3	8.3	1.6	7.5	7.6	7.6	7.8	7.8	7.9
		Dissolved Oxygen (mg/L)															
Observation Point	Depth\Month-Year	Oct-09		Nov-09		Dec-09		Jan-10		Feb-10		Mar-10		Apr-10		May-10	
The center of Imadsu-oki	0.5 m	8.7	9.2	9.4	10.0	10.4	10.5	9.8	9.7	10.6	11.1	11.6	12.0	12.0	12.1	11.3	10.6
	5 m	8.7	9.2	9.6	9.9	10.3	10.5	9.8	9.7	10.6	11.1	11.6	12.0	12.0	12.3	11.8	11.1
	10 m	8.5	9.0	9.4	9.9	10.2	10.5	9.8	9.6	10.5	11.0	11.6	11.9	12.0	12.4	11.6	10.9
	15 m	7.7	8.9	9.4	9.9	10.3	10.4	9.7	9.7	10.5	11.0	11.7	11.8	12.0	12.3	11.6	10.9
	20 m	5.9	7.5	8.8	9.8	10.3	10.4	9.7	9.6	10.5	11.0	11.6	11.8	11.9	12.1	11.6	10.6
	30 m	7.8	7.7	7.1	7.1	8.9	10.3	9.6	9.6	10.5	11.0	11.6	11.8	11.8	12.0	11.2	10.5
	40 m	8.1	8.6	7.3	6.8	7.3	9.3	9.1	10.1	10.5	11.0	11.2	11.6	11.8	11.8	11.0	10.3
	60 m	9.2	9.0	8.3	7.0	6.6	7.0	6.4	10.1	10.5	10.9	11.2	11.0	11.2	11.5	10.7	10.2
	80 m	6.9	7.6	7.2	5.8	4.1	5.2	5.6	6.9	10.4	11.2	11.0	10.9	10.1	10.6	9.9	9.2
	Bottom from 1 m	2.5	3.6	4.1	3.8	3.6	2.8	5.0	3.9	10.2	11.1	11.0	11.0	10.0	10.2	9.3	8.8
		Snow Water Equivalent (mm)															
Observation Point	Month-Year	Oct-09		Nov-09		Dec-09		Jan-10		Feb-10		Mar-10		Apr-10		May-10	
						12/1	12/2	1/9	1/21	2/8	2/22	3/5	3/22	4/2			
Yanagase	Mid-mountain areas					0	84	320	354	424	398	83	0	0			
Nakakawachi	Mountain areas					0	195	432	604	716	779	621	382	0			

[†] DO: dissolved oxygen. [‡] These measurements were conducted every two weeks at eight depths in the northern part of the lake at the center of Imadsu-oki (Figure 1; [36]). Observed average snow water equivalent at the north catchment area of Lake Biwa during the winter of 2009 (Figure 1).

4. Conclusions

We estimated the timescale of the response in Lake Biwa by calculating response functions. Spectral analysis was performed using the impulse response function technique with 30 year water-level and meteorological data to determine the average precipitation retention time of this lake. The response function of the precipitation water level was the strongest for the river inflow on approximately days 1–3, and the subsequent clear peaks appeared on days 25–35, 45, and 60–70. As for the calculated seasonal response function, the average precipitation retention time in the Lake Biwa catchment system was approximately 45 days. In addition, the precipitation retention time during the snowmelt season was shorter (i.e., 25–35 days) than that during the dry season (i.e., 60–70 days), except during the paddy irrigation season (May–August). Even though the precipitation retention time varied with seasons and surface conditions, according to the seasonal changes in the shape of the response function of the precipitation water level (and precipitation water volume), we conclude that the average precipitation retention time of the subsurface flow in Lake Biwa is approximately 45 days. Overall, the shape of the response function reflects the lake system, and this knowledge contributes to a better understanding of lake systems and can be helpful for lake resource managers. Moreover, inferring the delay time from

the response function may also be useful for determining the contribution of rainfall in increasing the water levels of other lakes.

Author Contributions: M.I. designed and analyzed the data and wrote the paper; Y.Y., T.T., C.J. and M.K. provided important suggestions for data analysis. All authors have read and agreed to the published version of the manuscript.

Funding: This research received no external funding.

Acknowledgments: We thank the Lake Biwa Work Office, the Ministry of Land Infrastructure, Transport, and Tourism (MLIT), General Affairs Division, the Waterworks Bureau City of Kyoto, the Kansai Electric Power Corporation, and the Japan Meteorological Agency, Lake Biwa Environmental Research Institute, White paper of Shiga Prefecture for providing data. We sincerely thank M. Sugiyama and Y. Furukawa of Kyoto University, K. Muraoka of the University of Waikato, Oizumi T. of Japan Agency for Marine–Earth Science and Technology (JMSTEC), Pedro Luiz Borges Chaffe of Federal University of Santa Catarina, and T. Mizuno of Lake Biwa Environmental Research Institute for their help with observation and comments on this study.

Conflicts of Interest: The authors declare no conflict of interest.

Appendix A

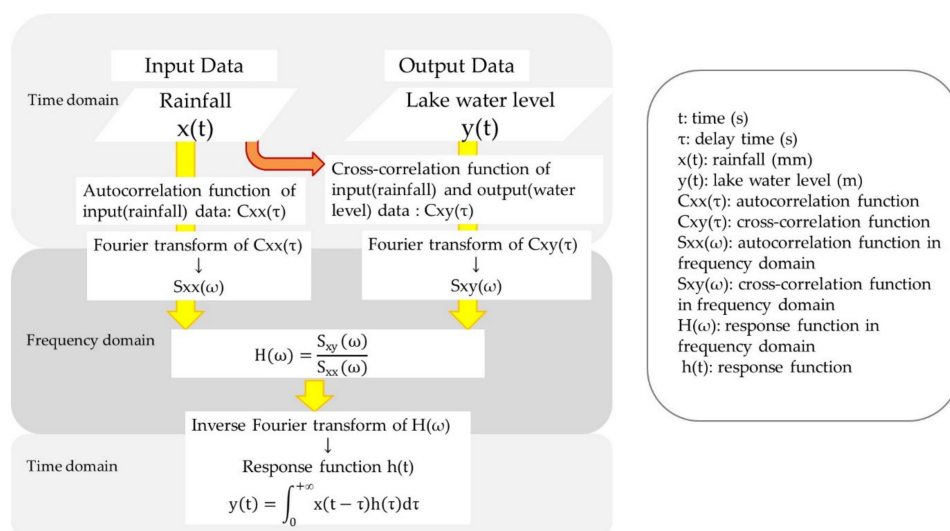


Figure A1. Flowchart for calculating the response function. Figure cited from [22].

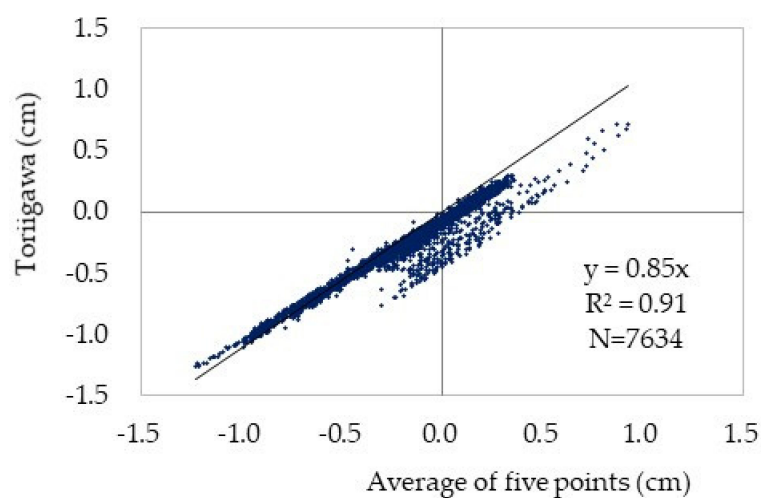


Figure A2. Relationship between Toriigawa and five points (Katayama, Omizo, Hikone, Katata, and Mihogasaki; Figure 1). BSL used the data of Toriigawa before 1992; after 1992, BSL used the average of five points.

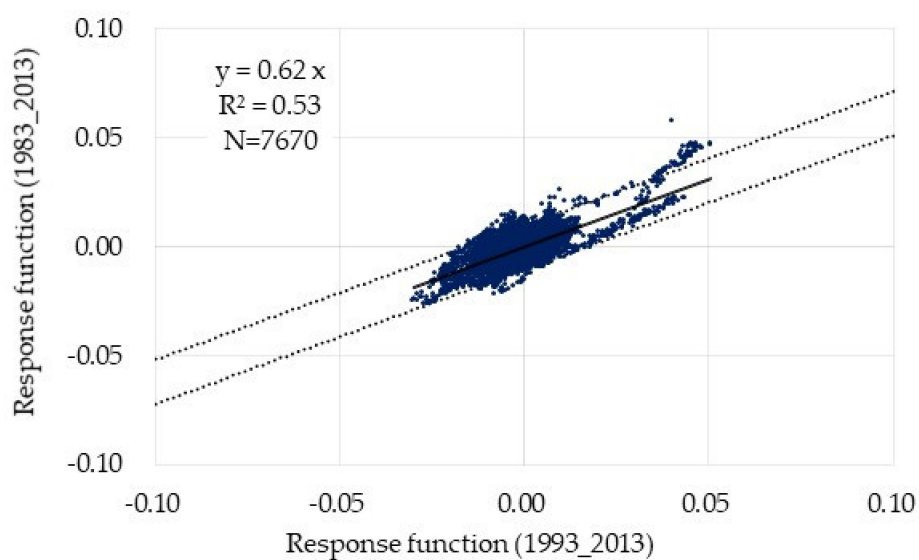


Figure A3. Relationship of calculated response functions from 1983 to 2013 and from 1993 to 2013. The dotted line represents the 95% confidence interval.

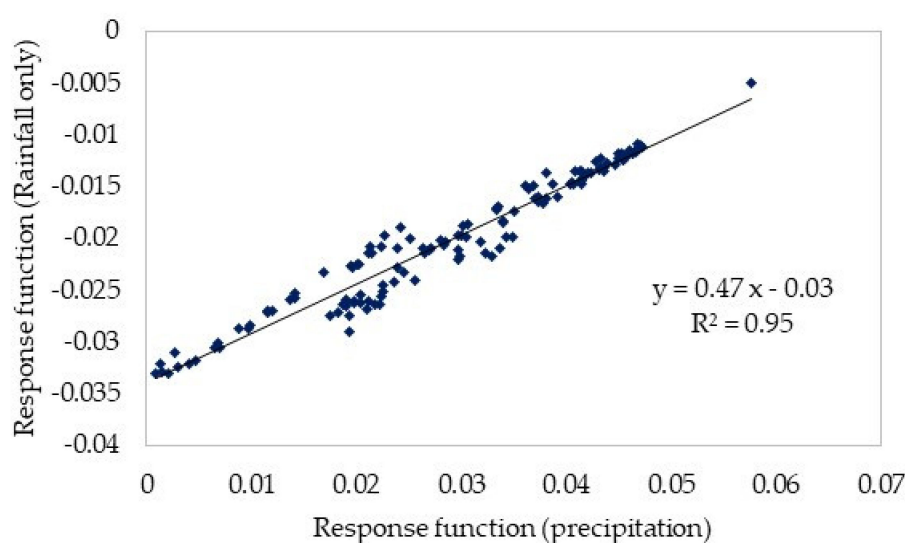


Figure A4. Relationship of the water-level response functions of rainfall water level and precipitation water level until day 131.

References

- Ostrovsky, I.; Rimmer, A.; Yacobi, Z.Y.; Nishri, A.; Sukenik, A.; Hadas, O.; Zohary, T. *Long-Term Changes in The lake Kinneret Ecosystem: The Effects of Climate Change and Anthropogenic Factors. Climatic Change and Global Warming of Inland Waters: Impacts and Mitigation for Ecosystems and SOCIETIES*; Goldman, R.C., Kumagai, M.M., Robarts, D.R., Eds.; John Wiley & Sons: West Sussex, UK, 2013; Volume 16, pp. 271–291.
- Micklin, P.P. Desiccation of the Aral Sea: A water management disaster in the Soviet Union. *Science* **1988**, *241*, 1170–1176. [[CrossRef](#)]
- Micklin, P.M. The Aral Sea disaster. *Annu. Rev. Earth Planet. Sci.* **2007**, *35*, 47–72. [[CrossRef](#)]
- Zohary, T.; Ostrovsky, I. Ecological impacts of excessive water level fluctuations in stratified freshwater lakes. *Inland Waters* **2011**, *1*, 47–59. [[CrossRef](#)]
- Wine, M.L.; Rimmer, A.; Laronne, J.B. Agriculture, diversions, and drought shrinking Galilee Sea. *Sci. Total Environ.* **2019**, *651*, 70–83. [[CrossRef](#)]
- AghaKouchak, A.; Norouzi, H.; Madani, K.; Mirchi, A.; Azarderakhsh, M.; Nazemi, A.; Nasrollahi, N.; Farahmand, A.; Mehran, A.; Hasanzadeh, E. Aral Sea syndrome desiccates Lake Urmia: Call for action. *J. Great Lakes Res.* **2015**, *41*, 307–311. [[CrossRef](#)]
- Alborzi, A.; Mirchi, A.; Moftakhari, H.; Mallakpour, I.; Alian, S.; Nazemi, A.; Hassanzadeh, E.; Mazdiyasn, O.; Ashraf, S.; Madani, K. Climate-informed environmental inflows to revive a drying lake facing meteorological and anthropogenic droughts. *Environ. Res. Lett.* **2018**, *13*. [[CrossRef](#)]
- Chaudhari, S.; Felfelani, F.; Shin, S.; Pokhrel, Y. Climate and anthropogenic contributions to the desiccation of the second largest saline lake in the twentieth century. *J. Hydrol.* **2018**, *560*, 342–353. [[CrossRef](#)]
- Khazaee, B.; Khatami, S.; Alemohammad, S.H.; Rashidi, L.; Wu, C.; Madani, K.; Kalantari, Z.; Destouni, G.; Aghakouchak, A. Climatic or regionally induced by humans? Tracing hydro-climatic and landuse changes to better understand the Lake Urmia tragedy. *J. Hydrol.* **2019**, *569*, 203–217. [[CrossRef](#)]
- Moore, J.N. Recent desiccation of Western Great Basin Saline Lakes: Lessons from Lake Abert, Oregon, U.S.A. *Sci. Total Environ.* **2016**, *554–555*, 142–154. [[CrossRef](#)] [[PubMed](#)]
- Tsai, C.; Miki, T.; Chang, C.W.; Ishikawa, K.; Ichise, S.; Kumagai, M.; Hsieh, C.H. Phytoplankton functional group dynamics explain species abundance distribution in a directionally changing environment. *Ecology* **2014**, *95*, 3335–3343. [[CrossRef](#)]
- Wantzen, K.M.; Rothhaupt, K.O.; Mörtl, M.; Cantonati, M.; G.-Tóth, L.; Fischer, P. Ecological effects of water-level fluctuations in lakes: An urgent issue. *Hydrobiologia* **2008**, *613*, 1–4. [[CrossRef](#)]
- Gownaris, N.J.; Rountos, K.J.; Kaufman, L.; Kolding, J.; Lwiza, K.M.M.; Pikitch, E.K. Water level fluctuations and the ecosystem functioning of lakes. *J. Great Lakes Res.* **2018**, *44*, 1154–1163. [[CrossRef](#)]
- Gronewold, A.D.; Rood, R.B. Recent water level changes across Earth's largest lake system and implications for future variability. *J. Great Lakes Res.* **2019**, *45*, 1–3. [[CrossRef](#)]
- Geraldes, A.M.; Boavida, M.J. Seasonal water level fluctuations: Implications for reservoir limnology and management. *Lakes Reserv. Res. Manag.* **2005**, *10*, 59–69. [[CrossRef](#)]
- Valdespino-Castillo, M.P.; Merino-Ibarra, M.; Jiménez-Contreras, J.; Fermín, S.; Castillo-Sandoval, S.F.; Ramírez-Zierold, A.J. Community metabolism in a deep (stratified) tropical reservoir during a period of high water-level fluctuations. *Environ. Monit. Assess.* **2014**, *186*, 6505–6520. [[CrossRef](#)] [[PubMed](#)]

17. Yang, J.; Lv, H.; Yang, J.; Liu, L.; Yu, X.; Chen, H. Decline in water level boosts cyanobacteria dominance in subtropical reservoirs. *Sci. Total Environ.* **2016**, *557–558*, 445–452. [[CrossRef](#)]
18. Mizuno, T.; Otuska, T.; Ogawa, M.; Funao, T.; Kanao, S.; Maehata, M. Spawning migration triggers in round crucian carp *Carassius auratus glandoculis* and water level fluctuations in Lake Biwa. *Jpn. J. Conserv. Ecol.* **2010**, *15*, 211–217. (In Japanese)
19. Sato, Y.; Nishino, M. Model analysis of the impact on spawning of cyprinid fishes by water level manipulation and prediction of the effect of measures. *Wetl. Res.* **2010**, *1*, 17–31. (In Japanese)
20. Fujioka, Y.; Taguchi, T.; Kikko, T. Spawning time, spawning frequency, and spawned egg number in a multiple-spawning fish, the honmoroko *Gnathopogon caerulescens*. *Nippon Suisan Gakkaishi* **2013**, *79*, 31–37. (In Japanese) [[CrossRef](#)]
21. Kikko, T.; Nemoto, M.; Ban, S.; Saegusa, J.; Sawada, N.; Ishizaki, D.; Nakahashi, T.; Teramoto, N.; Fujioka, Y. Efficient rearing of larvae and juveniles of Honmoroko *Gnathopogon caerulescens* in paddy fields. *Aquac. Sci.* **2013**, *61*, 303–309.
22. Iwaki, M.; Yamashiki, Y.; Muraoka, K.; Toda, T.; Jiao, C.; Kumagai, M. Effect of rainfall-influenced river influx on lake water levels: Time scale analysis based on impulse response function in the Lake Biwa catchment area. *Inland Waters* **2020**, *10*, 283–294. [[CrossRef](#)]
23. Iwaki, M.; Kumagai, M.; Jao, C.; Nishi, K. Evaluation of river inflows during heavy precipitation based on water level changes in a large lake. *Jpn. J. Limnol.* **2014**, *75*, 87–98. (In Japanese) [[CrossRef](#)]
24. Yokoki, H.; Kuwahara, Y.; Hanawa, N.; Gunji, M.; Tomura, T.; Hirayama, A.; Miura, N. Estimation of the future flood and inundation risk on Japanese major Rivers Basins caused by climate change. *Chikyu Kankyo Assoc. Int. Res. Initiat. Environ. Stud.* **2009**, *14*, 237–246. (In Japanese) [[CrossRef](#)]
25. Delbart, C.; Valdés, D.; Barbecot, F.; Tognelli, A.; Couchoux, L. Spatial organization of the impulse response in a karst aquifer. *J. Hydrol.* **2016**, *537*, 18–26. [[CrossRef](#)]
26. Hocking, M.; Kelly, B.F.J. Groundwater recharge and time lag measurement through Vertosols using impulse functions. *J. Hydrol.* **2016**, *535*, 22–35. [[CrossRef](#)]
27. Sakamoto, M.; Kumagai, M. *Lakes and Drainage Basins in East Asia Monsoon Area*; Nagoya University Press: Nagoya, Japan, 2006; p. 186. (In Japanese)
28. Haga, H. Confirmation of surface area of the southern basin of Lake Biwa Japan. *Jpn. J. Limnol.* **2006**, *67*, 123–126. (In Japanese) [[CrossRef](#)]
29. Muramoto, Y.; Michiue, M. Characteristics of alternating current between south and north basin in Lake Biwa. *Anu. Dis. Prev. Res. Inst. Kyoto Univ.* **1978**, *21*, 263–276. (In Japanese)
30. Fujino, Y. *Water Budget. An Introduction to Limnology of Lake Biwa*; Mori, S., Ed.; CiNii: Kyoto, Japan, 1980; pp. 19–26. (In Japanese)
31. Kawabata, H. Groundwater infiltration into the lake. *Environ. Sci. Res. Rep.* **1982**, *S704*, 29–36. (In Japanese)
32. Biwako Handbook. *Fluctuation of Lake Biwa*; The Editorial Committee of Biwako Handbook, Ed.; Shiga Prefecture: Shiga, Japan, 2010; p. 192. (In Japanese)
33. Kotoda, K. The estimation method of lake evaporation using climatological data. In *Report of the Hydraulic Experiment University of Tsukuba Environmental Research Center Papers*; University of Tsukuba: Tsukuba, Japan, 1977; pp. 53–65. (In Japanese)
34. Ikebuchi, S.; Seki, M.; Ohtoh, A. Evaporation from Lake Biwa. *J. Hydrol.* **1988**, *102*, 427–449. [[CrossRef](#)]
35. Iwaki, M. Estimation of the Distribution of Snow Water Equivalent in the North Catchment Area of Lake Biwa. Ph.D. Thesis, The University of Shiga Prefecture, Shiga, Japan, 2003.
36. Shiga Prefecture. *White Paper on the Environmental of Shiga Prefecture*; Shiga Prefecture: Shiga, Japan, 2010. (In Japanese)
37. Hidaka, K. *The Theory of Applied Integral Equation*; Kawakita Press: Tokyo, Japan, 1943. (In Japanese)
38. Hino, M. *Spectrum Analysis*; Asakura Press: Tokyo, Japan, 1977. (In Japanese)
39. Iwaki, M.; Hida, Y.; Ueno, K.; Saijyo, M. Observation of snow water equivalent in the North catchment area of Lake Biwa. *Lakes Reserv. Res. Manag.* **2011**, *16*, 215–221. [[CrossRef](#)]
40. Kumagai, M.; Fushimi, H. *Inflows Due to Snowmelt: Coastal and Estuarine Studies*; Okuda, S., Imberger, J., Kumagai, M., Eds.; The American Geophysical Union: Washington, WA, USA, 1995; Volume 48, pp. 129–139.
41. Chaffe, P.L.B.; Yamashiki, Y.; Takara, K.; Kato, M.; Iwaki, M. Influence of the Ane River Basin on Dissolved Oxygen Concentration of Lake Biwa: Sensitivity Study of the Biwa-3D model. *Anu. Dis. Prev. Res. Inst. Kyoto Univ.* **2010**, *53*, 91–96.
42. Chaffe, P.L.B.; Yamashiki, Y.; Takara, K.; Iwaki, M. A comparison of simple snowmelt models for the Ane River Basin. *Anu. Dis. Prev. Res. Inst. Kyoto Univ.* **2011**, *54*, 113–118.
43. Chaffe, P.L.B.; Yamashiki, Y.; Takara, K.; Iwaki, M. Measurement and modeling of the snowmelt in the Ane river basin. *J. Jpn. Soc. Civil Eng.* **2012**, *68*, 223–228. [[CrossRef](#)]